

Modulation of Photonic Crystals by Surface Acoustic Waves

M. M. de Lima, Jr.,^a P. V. Santos,^{a,c} R. Hey,^a and S. Krishnamurthy^b

^a*Paul-Drude-Institut für Festkörperelektronik, Hausvogteiplatz 5–7, 10117 Berlin, Germany*

^b*SRI International, Menlo Park, CA 94025, USA*

^c*Corresponding author: Tel: +49-30-20377-221; Fax: +49-30-20377-515; e-mail: santos@pdi-berlin.de*

Abstract

We demonstrate the dynamic control of light propagation in a one-dimensional photonic resonator by Rayleigh surface acoustic waves (SAW's) generated by interdigital transducers. The strong acoustic and optical fields in the resonator enhance the intensity of the Brillouin scattered light to values comparable to the one of the exciting beam. The SAW-driven resonator acts as a compact Bragg cell, which can be configured to operate as a switch, a frequency shifter, or a modulator.

Key words: photonic crystal, optical cavity, switch, modulator

PACS: 42.70.Qs, 42.65.Es, 42.79.Gn

1. Introduction

Among the several device geometries, which can be realized employing photonic crystals (PC's) [1,2], great attention has been directed towards active structures, which can dynamically control the light wavelength, polarization, or propagation direction through an external stimulus. Besides the fundamental interest, these structures are technologically important for the realization of tunable optical filters, modulators, and switches. Different concepts have been proposed to control the light flow in a PC by dynamically modifying the dielectric properties of its constituents. One of the ideas relies on the infiltration of PC's containing air holes with a liquid crystal [3]. Here, one explores the strong dependence of the refractive index of these materials on temperature and electric field. Shifts of the photonic band edges by approx. 2% induced by temperature changes have been reported [4]. The technologically more interesting tunability induced by an electric field, however, has so far been achieved only over a much narrower energy range [5]. Other approaches include modifications of the dielectric constants of a semiconductor through changes in

temperature or carrier density [6].

An alternative method to control light flow in PC's is based on the modulation by acoustic waves. This approach has been demonstrated in Bragg fibers with the acoustic wave propagating along the fiber axis [7]. More recently, a similar modulation procedure employing surface acoustic waves (SAW's) has been proposed for two-dimensional, semiconductor-based PC's [8]. The acoustic modulation has the advantage of being fast (time scales of less than a μs) in comparison with those induced by temperature. Due to the weakness of the elasto-optic interaction, however, long interaction paths between the light and acoustic waves and, thus, large device areas, become necessary to yield a sizeable modulation amplitude.

In this paper, we describe an active PC based on the modulation of a photonic cavity by a SAW, which is extremely compact and compatible with semiconductor technology. In this structure, the elasto-optical modulation of the cavity dielectric properties by the acoustic vibrations becomes strongly enhanced due to the concentration of the electromagnetic field in the cavity region. A gigantic enhancement of the cross section for Raman scattering by thermal optical phonons [9] as well as for Brillouin scattering by thermal acoustic

vibrations [10] in planar cavities have been previously reported. In the present design, the Brillouin scattering intensity is increased to values comparable to the incident beam by a high non-thermal population of SAW's generated by interdigital transducers (IDT's), which is employed to control the optical properties of the resonator. Finally, we show that the SAW-driven resonator acts as a compact Bragg cell with a thickness of less than $5 \mu\text{m}$, which can be configured to operate as a switch, a frequency shifter, or a modulator.

2. Sample Design

The one-dimensional PC resonator consists of a $\lambda/2$ optical cavity (C) surrounded by Bragg mirrors (BM_1 and BM_2), as illustrated in Fig. 1. The resonance condition is achieved when the vertical component of the light wave vector k_z is equal to $k_c = 4\pi n_c/d_c$, where d_c and n_c denote the thickness and the refractive index of the cavity layer, respectively. For normal incidence, the resonance wavelength becomes $\lambda_c = 2\pi/k_c$. The structure was monolithically grown on a GaAs (001) substrate using molecular-beam epitaxy. The lower Bragg mirror BM_1 is composed of 15 periods, each containing a $\lambda/4$ AlAs and a $\lambda/4$ GaAs layer. The first 5 periods of the upper mirror BM_2 are identical to those in BM_1 , in the remaining 5 periods, which are located adjacent to the cavity, the thickness of the GaAs layers was increased to $3\lambda/4$.

The optical modulation by the SAW is mediated by three mechanisms. The first comprises the conventional elasto- and electro-optical modifications of the refractive index by the SAW strain and piezoelectric fields, respectively. For wavelengths away from electronic transitions, which will be the case discussed here, the elasto-optic contribution (Δn_{eo}) normally dominates over the electro-optic one. The second mechanism results from the modulation of the layer thicknesses by the vertical strain component $u_{zz} = \partial u_z / \partial z$ of the SAW displacement field \mathbf{u} . To first order approximation, which neglects the depth dependence of the SAW fields, the variation $\Delta \lambda_c$ of the resonance wavelength becomes

$$\frac{\Delta \lambda_c}{\lambda_c} = -\frac{\Delta n_c}{n_c} = -\left[\frac{\Delta n_{eo}}{n_c} + u_{zz} \right]. \quad (1)$$

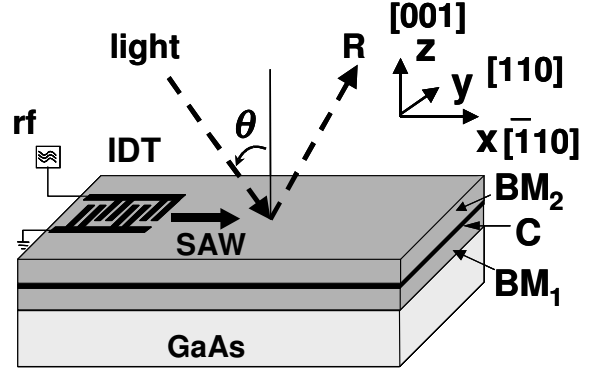


Fig. 1. Structure of the optical resonator, which is composed of two Bragg mirrors BM_1 and BM_2 and a cavity C monolithically grown on a GaAs (001) substrate. SAW's propagating along $x = [\bar{1}10]$ are generated by an interdigital transducer (IDT) placed on top of the layer stack. θ denotes the incident angle.

The third mechanism is associated with the modulation of the interface profiles by the SAW displacement field, thus creating a structural grating for the incident light. An important feature of the acoustic modulation resides in the fact that the modulation of the thicknesses [expressed by u_{zz} in Eq. (1)] and of the interface profiles can be substantially larger than the elasto-optic one.

The optical resonators were projected to operate at optic wavelengths λ_c between 900 and 1000 nm employing a SAW with wavelength $\lambda_{\text{SAW}} = 5.6 \mu\text{m}$. In the design of the layer structure one has to take into account the depth dependence of the SAW strain field. Figure 2 shows numerical calculations of the strain component u_{zz} (diamonds) as well as of Δn_{eo} for light polarization in the direction perpendicular (dots) and parallel (circles) to the SAW propagation direction x . The calculations were performed for the structure given in Fig. 1 assuming $\lambda_c = 1000 \text{ nm}$ and a SAW linear power density $P_l = 200 \text{ W/m}$ (P_l is defined as the acoustic power flux per unit length along the cross section of the SAW beam). For the perpendicular polarization (y -polarization), $\Delta n/n$ reaches its maximum modulation amplitude of 5.5×10^{-4} for depths between $0.25\lambda_{\text{SAW}}$ and $0.45\lambda_{\text{SAW}}$. Approximately two-thirds of $\Delta n_c/n_c$ in Eq. (1) is accounted for by the strain contribution u_{zz} , thus demonstrating its dominating role over the elasto-optic contribution. The latter, however, makes the modulation amplitude dependent on light wavelength and polarization. For light polarized along x , a

smaller value for $\Delta n_c/n_c$ is obtained, since in this case the elasto-optic contribution in Eq. (1) has the opposite sign as the strain one. The cavity position (indicated by the arrows) was selected to maximize $\Delta n_c/n_c$ and, at the same time, to allow for thick BM stacks, in order to increase the quality factor Q .

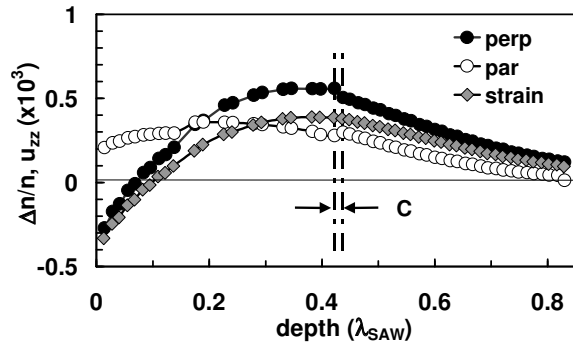


Fig. 2. Modulation of the strain (u_{zz} , diamonds) and of the refractive index ($\Delta n/n$) for light polarized parallel (circles) and perpendicularly (dots) to the SAW propagation direction, as a function of depth. The position of the cavity (C) within the layer stack is also indicated.

3. Results

The reflectivity of the resonator was measured using the radiation of a super-luminescent diode polarized along y and an optical spectrum analyzer as the detector. The solid line in Fig. 3(a) displays the resonator reflectivity for normal incidence R_0 , recorded using an objective with a small numerical aperture ($f/0.055$) to focus and collect the reflected light, in order to ensure a narrow distribution of the angles of incidence. For the cavity, $Q = 800$, which is essential for enhancing the electromagnetic fields in the cavity region and, consequently, the acoustic modulation. Outside the resonance range, the reflectivity was found to be comparable to that of a silver mirror with nominal reflectivity of 0.98 ± 0.02 and therefore, assumed to be unity within the experimental resolution.

The dynamic control of the resonator is based on the modulation of the resonance frequency (cf. Eq. 1) by the SAW. The latter is demonstrated by the time-resolved reflectivity traces displayed in Fig. 3(b). The reflectivity R , which is normalized to its average (dc) value R_{dc} , was measured by focusing the incident beam

onto a spot with dimensions smaller than $\lambda_{\text{SAW}}/2$ using a wide-aperture objective ($f/0.42$), in order to probe the local changes in the cavity optical properties induced by the SAW [cf. inset of Fig. 3(c)]. The dots and circles were recorded for the wavelengths $\lambda_+ > \lambda_c$ and $\lambda_- < \lambda_c$ around λ_c indicated, respectively, by the dashed and solid arrows in Fig. 3(c). The reflectivity traces are modulated with the frequency of the SAW ($f_{\text{SAW}} = 537$ MHz) and phase-shifted by 180° with respect to each other. The phase shift reflects the fact that the modulated resonance wavelength approaches the detection one at opposite half cycles of the SAW. The spectral dependence of the modulation amplitude ΔR and its phase are shown by the circles and squares in Fig. 3(c), respectively. The modulation amplitude is maximal at the flank wavelengths and almost vanishes at the cavity resonance λ_c . In fact, only a modulation at $2f_{\text{SAW}}$ is expected at this wavelength. The peak modulation amplitude ($\Delta R/R_{dc}$) reaches values of up to 15%.

The light scattering process responsible for the modulation requires the conservation of energy and momentum. The latter, however, is relaxed in the plots of Figs. 3(b) and 3(c) due to the wide range of incident angles provided by the wide-aperture objective. When the measurements are performed under normal incidence employing a collimated beam, however, only small changes in the dc reflectivity are observed, as shown by the dashed line in Fig. 3(a). A more favorable situation for light control is achieved if the resonator is illuminated at an angle of incidence θ satisfying the Bragg condition $\theta = \theta_B = \arctan[\lambda_c/(2\lambda_{\text{SAW}})]$, as illustrated in the left inset of Fig. 4. In this case, momentum conservation is ensured with the first-order diffraction beam (indicated by k_1) propagating in the opposite direction as the incident beam. Figure 4 displays the intensity $R(\theta)$ of the beam reflected in the opposite direction as the input beam (see left inset) as a function of θ . The corresponding peak intensity is displayed as a function of θ in the right inset. The diffraction intensity reaches its maximum of approx. 15% for $\theta_B = 4.7^\circ$, which are close to the values of 19% and 5.0° , respectively, calculated by a numerical model based on Eq. 1. Values of $R(\theta)$ of up to 40% were obtained for by improving the rf coupling to the IDT's.

The configuration of Fig. 4 with $\theta = \theta_B$ turns the resonator into a versatile Bragg cell, which can be operated as a frequency shifter, a switch, as well as a

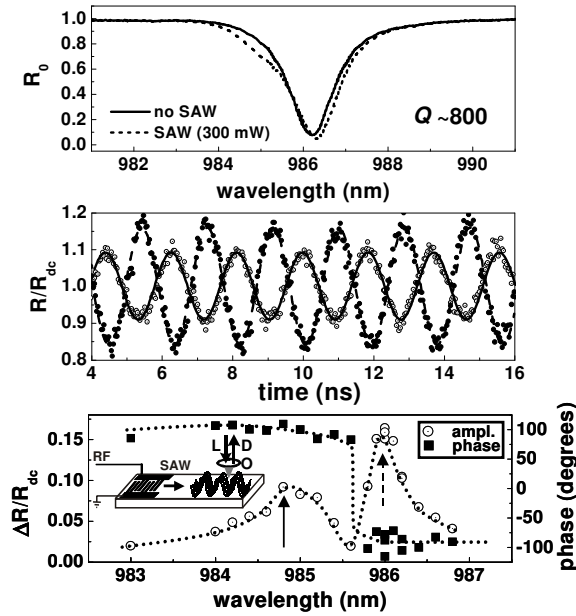


Fig. 3. (a) Normal incidence reflectivity of the cavity resonator (R_0) in the absence (solid line) and under a SAW with power density $P_l = 300 \text{ W/m}$ (dashed line). The quality factor Q of the cavity (without SAW excitation) is approx. 800. (b) Time-resolved reflectivity R normalized to the average (dc) value R_{dc} . The solid and open circles were recorded at the wavelengths indicated by the dashed and solid vertical arrows in (c), respectively. (c) Wavelength dependence of the normalized amplitude ($\Delta R/R_{dc}$) and phase of the reflectivity at the SAW frequency. The measurement configuration is shown in the inset. The spectra in (b) and (c) were recorded with $P_l = 150 \text{ W/m}$.

modulator. The frequency shifting action arises automatically from the up-shift of the diffracted beam by $+\omega_{\text{SAW}}$ required by energy conservation. Switching with a high on/off contrast is accomplished by simply turning the IDT on and off. Finally, the operation as a modulator is realized by modulating the rf voltage applied to the IDT with the information signal. Note that modulation action is also accompanied by a frequency shift ω_{SAW} , a feature which can be explored for wavelength multiplexing applications.

4. Conclusion

In conclusion, we have demonstrated that strong acoustic and light fields in one-dimensional photonic resonators lead to Brillouin scattering intensities com-

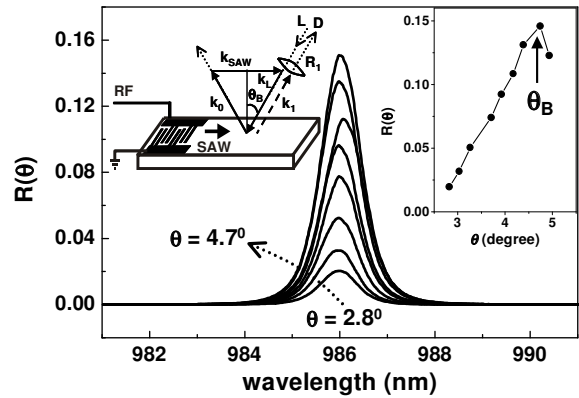


Fig. 4. Angular dependence of the reflectivity $R(\theta)$ measured in the configuration illustrated in the left inset for $P_l = 300 \text{ W/m}$. The right-side inset displays the reflectivity maximum as a function of θ . The Bragg condition sketched on the left inset is fulfilled for $\theta = \theta_B = 4.7^\circ$.

parable to the one of the exciting beam. SAW-driven resonators based on this principle can be employed as photonic switches, frequency shifters, and modulators fabricated monolithically on GaAs.

We thank H. T. Grahn for comments and for a critical reading of the manuscript as well as S. Krauß and W. Seidel for the preparation of the samples. Partial support from the Deutsche Forschungsgemeinschaft is gratefully acknowledged.

References

- [1] S. John, Phys. Rev. Lett. 58 (1987) 2486.
- [2] E. Yablonovitch, Phys. Rev. Lett. 58 (1987) 2059.
- [3] K. Busch and S. John, Phys. Rev. Lett. 83 (1999) 967.
- [4] K. Yoshino, Y. Shimoda, Y. Kawagishi, K. Nakayama, and M. Ozaki, Appl. Phys. Lett. 75 (1999) 932.
- [5] D. Kang, J. E. Maclennan, N. A. Clark, A. A. Zakhidov, and R. H. Baughman, Phys. Rev. Lett. 86 (2001) 4052.
- [6] P. Halevi and F. Ramos-Mendieta, Phys. Rev. Lett. 85 (2000) 1875.
- [7] P. S. J. Russell, Phys. Rev. Lett. 56 (1986) 596.
- [8] P. V. Santos, J. Appl. Phys. 89 (2001) 5060.
- [9] A. Fainstein, B. Jusserand, and V. Thierry-Mieg, Phys. Rev. Lett. 75 (1995) 3764.
- [10] M. Trigo, A. Bruchhausen, A. Fainstein, B. Jusserand, and V. Thierry-Mieg, Phys. Rev. Lett. 89 (2002) 227402.